IEEE Access
Multidisciplinary | Rapid Review | Open Access Journal

Received 9 October 2022, accepted 25 October 2022, date of publication 14 November 2022, date of current version 21 February 2023.

Digital Object Identifier 10.1109/ACCESS.2022.3222069

RESEARCH ARTICLE

Bipartite Synchronization of Multi-Agent Systems With Signed Graph Under Deception Attacks and Application in Speech Communication

YANSEN LIU, SUYING SHENG, JIAHAO ZHANG, AND GUOPING LU
School of Electrical Engineering, Nantong University, Nantong, Jiangsu 226019, China

Corresponding author: Guoping Lu (lu.gp@ntu.edu.cn)

This work was supported in part by the National Natural Science Foundation of China under Grant 62073180, in part by the Doctoral Research Startup Fund Project of Nantong University, and in part by the Postgraduate Research & Practice Innovation Program of Jiangsu Province under Grant KYCX22_3348.

ABSTRACT This paper addresses the bipartite synchronization of multi-agent systems with time-varying delays and signed graph under deception attacks, where the systems contain both the self-structure delayed term and the coupling delayed term. The deception attacks are assumed to be randomly launched at each impulse instant. By using the gauge transformation, Lyapunov function method, Halanay differential inequality and linear matrix inequality techniques, several sufficient conditions are newly established to guarantee the achievement of bipartite synchronization, in which some special cases of multi-agent systems without delay or deception attacks are further considered. Two numerical examples are provided to illustrate the effectiveness of the proposed results. Finally, a new multi-agent speech communication system is constructed based on the bipartite synchronization of the multi-agent systems, where two agents for point-to-point communication can generate synchronous chaotic encryption/decryption key streams. The experimental results show that the proposed multi-agent speech communication system has the advantages of high security against some classical attacks.

INDEX TERMS Multi-agent systems, bipartite synchronization, signed graph, deception attacks, speech communication.

I. INTRODUCTION

A multi-agent system [1], [2] refers to a computing system composed of multiple agents interacting with each other in a certain environment, in which any agent can interact to complete more complex work. In recent years, multi-agent systems have become a research hotspot in the field of control and artificial intelligence. The cooperative control of multi-agent systems is a hot research topic in the field of control. The cooperative control of multi-agent systems includes consensus control, rendezvous control, coalescence control, and formation control. The latter three can be regarded as the generalization and special cases of consensus control. The collaborative control of multi-agent systems has achieved extensive research results in the past 20 years. For example, information flow and formation coordination control of vehicles [3], distributed vehicle coordination control with local information exchange [4], cooperative control of multi-agent systems and its application in unmanned vehicles [5].

In a multi-agent system, some agents track a given target or agent, which is called leader-following consistency phenomenon. The agent that plays a leading role in a multi-agent system is called the leader, and the rest of the agents that need to follow the leader are called followers [6]. Leader-following consistency means that the agents in the system communicate and coordinate with each other, so that the state values of all follower agents change with time, and finally track the state value of the leader agent. Leader-follower consistency, on the one hand, it can simplify the design and implementation of the control system, on the other hand, it can further save energy and control costs.

The associate editor coordinating the review of this manuscript and approving it for publication was Yichuan Jiang.

While in the leaderless-following system, there must be information transmission and reception between each agent, and the consistency of the system depends on the interaction between all agents. That is, only through the joint action of all agents can all state variables of the system be consistent. The leaderless-following consistency has higher requirements on the design and imple-mentation of the control system, and the control cost is relatively large, but the control effect is more precise than the leader-following system.

Multiple agents need to transmit information through the network. The traditional network model is generally an undirected graph or a directed graph. A node of the network represents a single agent, and the edges with positive weights between nodes represent the communication between two agents. The above-mentioned network model is an unsigned network. However, with the further development of network research, we find that traditional unsigned networks cannot accurately describe some oppositional relationships in real society. For example, in the medical field, there is a relationship of promotion and antagonism between drugs, and in the field of society, there is a relationship of trust and distrust in the communication between people. Therefore, in the multi-agent systems [7], [9], [30], [31], there will also be a certain cooperation and opposition between agents. In view of the above situation, the concept of signed graph is introduced [8], [9], where the weight of the edge in the signed graph is no longer limited to be positive, but can also be negative. An edge with a positive weight represents a cooperative relationship between the two agents, while an edge with a negative weight represents an antagonistic relationship. Therefore, the research on multi-agent systems is no longer limited to unsigned networks, but gradually extended to the signed network. Synchronization is considered to be one of the most important phenomena in complex dynamic network theory, and has important applications in a variety of physical, biological and technological systems [10]. Thus, the research on synchronization of signed network has attracted extensive attention of researchers. Altafni first put forward the concept of bipartite synchronization of signed networks, that is, the states of nodes would eventually converge to two parts with the same and opposite modulus [11], [12], where the consistency problem of signed network was transformed into a classical consistency problem only under the condition of balanced network structure. At present, there are many control methods to realize the bipartite synchronization of multi-agent systems with signed graph, such as state feedback control [13], sliding mode control [14], distributed control [15], intermittent control [16] and so on. Among them, there are many researches on pinning control, which sets key nodes and designs controllers to achieve control effect. In [17] and [18], the pinning control strategy is adopted to realize the bipartite synchronization of multi-agent systems with signed graph. So far, based on different signed network models, some achievements have been made in the research of bipartite synchronization, including bipartite synchronization of Lur'e Networks [19] and bipartite synchronization for signed networks of harmonic oscillator systems [20]. Especially in [20], the communication delay of the network is considered and the convergence of the network is analyzed. In addition, Meng [21] studied the problem of bipartite containment tracking of signed networks, and Hu and Yu [22] adopted a time-delay control method to study the consensus problem of multi-agent systems in the cooperation-competition network with inherent nonlinear dynamics. In [23], Parastesh and Rajagopal et al. studied the synchronization of networks with linear diffusive coupling and proposed that the stability of the synchronous solution depends only on the average coupling and not on the instantaneous coupling. In [24], a modified signed-susceptible-infectious-susceptible epide-miological model was proposed to study the dynamics of epidemic spreading on signed networks.

The multi-agent systems with signed graph will be affected by the delay. On the one hand, there is a time delay in the multiple agent itself, and the calculation of the devices in the system needs to consume a certain time. On the other hand, due to the limited transmission speed, transmission congestion and transmission delay are also normal phenomena, which will lead to divergence and oscillation, and the network system will be unstable, further reducing the performance of network information transmission. Bipartite synchronization of signed networks under transmission delay has recently attracted great interest in [25] and [26]. In [25], the problem of bipartite consensus was studied for multi-agent systems with antagonistic interactions and communication delays. In [26], the problem of exponential bipartite synchronization was studied for delayed signed networks with multi-links by aperiodically intermittent control. In addition to the impact of time delay, there are also security risks in the data transmission process, and the network control process is vulnerable to malicious attacks. As a way of network attack, deception attack will have a bad impact on the information interaction on the network. Deception attack means that correct information such as the output signal of the controller and the measurement signal of the sensor are tampered by the attacker and the wrong information is transmitted to the network. In response to the above phenomenon, people have studied the bipartite synchronization of multi-agent systems under the deception attacks. In [27], the sampling-based leaderless consensus problem for nonlinear multi-agent systems under deception attacks is studied by using the decoupled method. In [28], based on impulse control, the secure synchronization of multi-agent systems under deception attack is studied. In [29], the fault-tolerant secure consensus tracking problem of nonlinear multi-agent systems with deception attacks and uncertain parameter delays is investigated under the impulse control framework. To the best of our knowledge, there have been few available results on bipartite synchronization of multi-agent systems with signed graph and deception attack considering both the self-structure delayed term and the coupling delayed term, which motivates the research in this paper.

Although there has been some progress in the application of bipartite synchronization of multi-agent systems, it is less

reported in the field of secure communication. At the same time, chaotic signal is a natural cryptography signal because of its own pseudo-random characteristics. In this paper, we try to make use of the multi-agent system composed of nodes with chaotic dynamics to generate chaotic key streams, which can be applied in the speech communication based on its bipartite synchronization.

The contributions of this paper are summarized as follows.

- Firstly, the influence of self-structure delay, transmission delay and deception attack are simultaneously considered in the multi-agent systems with signed graph.
- Secondly, several sufficient conditions are newly established to guarantee the achievement of bipartite synchronization, in which some special cases of multi-agent systems without delay or deception attacks are further considered, by using the gauge transformation, Lyapunov function method, Halanay differential inequality and linear matrix inequality techniques.
- Thirdly, based on the bipartite synchronization results of multi-agent systems, a new chaotic multi-agent speech secure communication system is constructed to verify the feasibility of the proposed theoretical method.

The rest of the paper is arranged as follows. In Section II, some preparations are given and the bipartite synchronization problem of signed networks under self-delay, transmission delay and deception attacks is proposed. Section III proposes the sufficient conditions for the bipartite synchronization of the signed network and gives the relevant proof process. Section 4 further demonstrates the theoretical results through two numerical simulations. The fifth section is the specific application of the theoretical results of this paper. A new chaotic voice secure communication system is constructed to verify the feasibility of the proposed theoretical method. Finally, in Section VI, the relevant conclusions of this paper are given.

Notations: I_N represents an $N * N$ identity matrix, and 0 means zero matrix. $\lambda_{\min}(A)$ and $\lambda_{\max}(A)$ denote the minimum and maximum eigenvalues of matrix A, respectively. $\otimes$ represents the Kronecker product of the matrix. $E\{x\}$ is the expectation of the random variable x. $\Pr ob\{\ldots\}$ represents the probability of an event occurring. $A > 0$ means that matrix A is a positive definite matrix.

II. PRELIMINARIES AND PROBLEM FORMULATION

A. SIGNED GRAPH THEORY

A signed graph consisting of N nodes can be represented by a triple combination $\mathcal{G} = \{\mathcal{N}, \varepsilon, \mathcal{A}\}$, where $\mathcal{N} = \{1, 2, \ldots, N\}$ is the node set, $\varepsilon \subseteq \mathcal{N} \times \mathcal{N}$ is the edge set, and $\mathcal{A} = \left(a_{ij}\right)_{N\times N}$ denotes the adjacency matrix of signed graph. $a_{ij} \neq 0 (i \neq j) \Leftrightarrow (i, j) \in \varepsilon$, that is, there exists a directed edge from node j to node i. It is assumed that signed graph $\mathcal{G}$ doesn't contain any self-loop ($a_{ii} = 0, i \in \mathcal{N}$). When $\mathcal{G}$ is a directed graph, $a_{ij} > 0$ indicates that the relationship from node j to node i is cooperative, while $a_{ij} < 0$ means that there is a competitive relationship from node j to node i [19], [20], [30].

The Laplacian matrix $L = (l_{ij})_{N\times N}$ in signed graph $\mathcal{G}$ is given as follows:

$$L = D - \mathcal{A} \tag{1}$$

where $D = diag(d_1, d_2, \ldots d_N)$, $d_i = \sum_{j=1, j\neq i}^{N} \left|a_{ij}\right|$, $i \in \mathcal{N}$.

Remark 1: It is worth mentioning that the Laplacian matrix L associated with a signed graph $\mathcal{G}$ is not necessarily a zero-row sum matrix. One can easily get that the i-th row sum of L is $\sum_{j=1, j\neq i}^{N} \left|a_{ij}\right| - \sum_{j=1, j\neq i}^{N} a_{ij}$. It is obvious that if there exists $j \in \{1, 2, \cdots, N\}$ that satisfies $a_{ij} < 0$, then L is not a zero-row sum matrix due to $\sum_{j=1}^{N} l_{ij} \neq 0$, which is quite different from the traditional Laplacian matrix in unsigned networks.

Definition 1 [8], [20]: A signed graph $\mathcal{G}$ is said to be structurally balanced, if the nodes of signed graph are divided into two cluster $\mathcal{N}_1$ and $\mathcal{N}_2$, $\mathcal{N}_1 \cup \mathcal{N}_2 = \mathcal{N}$, $\mathcal{N}_1 \cap \mathcal{N}_2 = \emptyset$, such that $a_{ij} > 0, \forall i, j \in \mathcal{N}_p (p \in [1, 2])$ and $a_{ij} \leq 0, \forall i \in \mathcal{N}_p$, $j \in \mathcal{N}_q (p \neq q; p, q \in [1, 2])$. Otherwise it is structurally unbalanced.

B. PROBLEM FORMULATION

Consider the multi-agent system consisting of N agents, which is subject to time-varying delay and deception attacks, each agent can be regarded as a node:

$$\begin{cases} \dot{x}_i(t) = A_1 x_i(t) + A_2 x_i(t - \tau(t)) + B_1 f(x_i(t)) \\ +B_2 f(x_i(t - \tau(t))) - \alpha \sum_{j=1}^{N} \left|g_{ij}\right| (x_i(t) - sign(g_{ij}) x_j(t)) \\ -\beta \sum_{j=1}^{N} \left|g_{ij}\right| (x_i(t - \tau(t)) - sign(g_{ij}) x_j(t - \tau(t))), t \neq t_p, \\ \Delta x_i(t_p) = \rho(t_p) \psi(x_i(t_p^-)), p \in \mathbb{N}^+. \end{cases} \tag{2}$$

where $x_i(t) = (x_{i1}(t), x_{i2}(t), \ldots, x_{in_x}(t))^T \in \mathbb{R}^{n_x} (i \in \mathcal{N})$ represents the state vector of the *ith* node at time t. $f(x_i(t)) = (f_1(x_{i1}(t)), f_2(x_{i2}(t)), \ldots, f_{n_x}(x_{in_x}(t)))^T \in \mathbb{R}^{n_x}$ is a nonlinear function. $A_1, A_2, B_1, B_2 \in \mathbb{R}^{n_x \times n_x}$ are constant matrices. $\tau(t)$ denotes the time-varying delay. It is assumed that $0 < \tau(t) < \bar{\tau}$ with $\bar{\tau} > 0$ being a constant. and β are the coupling strengths with $\alpha > 0$ and $\beta > 0$. g_{ij} represents the (i, j)-th entry of the adjacency matrix associated with the underlying signed graph $\mathcal{G}$ of system (2). $\{t_p\}_{p=0}^{\infty}$ is the equispaced impulsive time sequence satisfying $0 = t_0 < t_1 < t_2 < \cdots < t_p < \cdots$. It is assumed that the impulsive interval $t_p - t_{p-1} = h, p = 1, 2, \cdots$, where $h > 0$ is a known constant. $\Delta x_i(t_p) = x_i(t_p) - x_i(t_p^-) = x_i(t_p^+) - x_i(t_p^-) = \lim_{t\to t_p^+} x_i(t) - \lim_{t\to t_p^-} x_i(t)$. Similarly to [32], it is assumed that deception attacks randomly launch at each impulse instant. $\psi(x_i(t)) \in \mathbb{R}^{n_x}$ represents a deception attack signal. The Bernoulli distribution sequence $\{\rho(t_p), p \in \mathbb{N}^+\}$ takes values 0 and 1 with probability

$\Pr ob\{\rho(t_p) = 1\} = \bar{\rho}$ and $\Pr ob\{\rho(t_p) = 0\} = 1 - \bar{\rho}$, where $\bar{\rho}$ is a constant and $0 < \bar{\rho} < 1$.

Remark 2: The non-delayed coupling term $\alpha \sum_{j=1}^{N} \left|g_{ij}\right| (x_i(t) - sign(g_{ij}) x_j(t))$ and the delayed coupling term $\beta \sum_{j=1}^{N} \left|g_{ij}\right| (x_i(t - \tau(t)) - sign(g_{ij}) x_j(t - \tau(t)))$ are simultaneously considered in system (2). In addition, the dynamic

system itself also considers the influence of the time-varying delay $\tau(t)$. In addition, if the time-varying delay $\tau(t)$ is ignored, that is, $A_2 = B_2 = 0$ in (2), and $\beta = 0$ in (2), and the influence of deception attacks is not considered.

Remark 3: In [32], it is pointed out that a physical attack may cause $x_i(t)$ to change suddenly at t_p. This phenomenon is mathematically described as impulsive disturbance in the system (2). In addition, it is assumed that deception attacks occur randomly at each impulse moment, and the Bernoulli distribution sequence is used to describe the random occurrence of deception attacks [27].

Applying the Laplacian matrix L, the multi-agent system can be rewritten as:

$$\begin{cases} \dot{x}_i(t) = A_1 x_i(t) + A_2 x_i(t-\tau(t)) + B_1 f(x_i(t)) \\ +B_2 f(x_i(t-\tau(t))) - \alpha \sum_{j=1}^{N} l_{ij} x_j(t) \\ -\beta \sum_{j=1}^{N} l_{ij} x_j(t-\tau(t)), t \neq t_p, \\ \Delta x_i(t_p) = \rho(t_p)\psi(x_i(t_p^-)), p \in \mathbb{N}^+. \end{cases} \tag{3}$$

Assumption 1: For any $m \in \{1, 2, \ldots, n_x\}$, $f_m(x_{im}(t))$ is an odd function and satisfies the following inequality:

$$|f_m(x) - f_m(y)| \leq \nu_m |x - y|, \quad \forall x, y \in R$$

where ν_m is a given constant and $\nu_m > 0$.

Assumption 2: $\psi(x_i(t))$ is an odd function, $\psi(x_i(t)) \in R^{n_x}$ satisfies the following inequality:

$$\|\psi(a) - \psi(b)\| \leq \theta \|a - b\|, \quad \forall a, b \in R^{n_x}$$

where θ is a given constant and $\theta > 0$.

Assumption 3 [18], [19], [20]: The signed graph $\mathcal{G}$ is structurally balanced.

Assumption 4 [18], [19]: The signed graph $\mathcal{G}$ contains a directed spanning tree.

Definition 2: Under Assumption 3, the multi-agent system with signed graph is considered to achieve bipartite synchronization if satisfy: $\lim_{t\to\infty} \mathrm{E}\left\{\|\omega_i x_i - \omega_1 x_1\|^2\right\} = 0$ for any $\forall i \in \mathcal{N}(i \neq 1)$, where $\omega_i = 1(i \in \mathcal{N}_1)$ and $\omega_i = -1(i \in \mathcal{N}_2)$.

Let

$$\bar{x}_i = \omega_i x_i, \omega_i \in \{1, -1\}, x_i = \omega_i \bar{x}_i.$$

According to assumptions 1 and 2, $f_m(x_{im}(t))$ and $\psi(x_i(t))$ are odd functions, and the multi-agent system (3) becomes the following form:

$$\begin{cases} \dot{\bar{x}}_i(t) = A_1 \bar{x}_i(t) + A_2 \bar{x}_i(t-\tau(t)) + B_1 f(\bar{x}_i(t)) \\ +B_2 f(\bar{x}_i(t-\tau(t))) - \alpha \sum_{j=1}^{N} \bar{l}_{ij} \bar{x}_j(t) \\ -\beta \sum_{j=1}^{N} \bar{l}_{ij} \bar{x}_j(t-\tau(t)), t \neq t_p \\ \Delta \bar{x}_i(t_p) = \rho(t_p)\psi(\bar{x}_i(t_p^-)), p \in \mathbb{N}^+. \end{cases} \tag{4}$$

where $\bar{l}_{ij} = \omega_i l_{ij} \omega_j = -|g_{ij}| (i \neq j)$, $\bar{l}_{ii} = \sum_{j=1, j\neq i}^{N} |g_{ij}|$.

Denote:

$$e_i(t) = \bar{x}_i(t) - \bar{x}_1(t), e(t) = \left[e_1^T(t), \ldots, e_N^T(t)\right]^T,$$

$$\eta_i(t) = f(\bar{x}_i(t)) - f(\bar{x}_1(t)), \eta(t) = \left[\eta_1^T(t), \ldots \eta_N^T(t)\right]^T,$$

$$\varphi_i(t) = \psi(\bar{x}_i(t)) - \psi(\bar{x}_1(t)), \varphi(t) = \left[\varphi_1^T(t), \ldots, \varphi_N^T(t)\right]^T,$$

After applying the Kronecker product, the system (4) is further transformed into the following:

$$\begin{cases} \dot{e}(t) = D_\alpha e(t) + (I_{N-1} \otimes B_1)\eta(t) + D_\beta e(t-\tau(t)) \\ +(I_{N-1} \otimes B_2)\eta(t-\tau(t)), t \neq t_p, \\ \Delta e(t_p) = \rho(t_p)\varphi(t_p^-)), p \in \mathbb{N}^+. \end{cases} \tag{5}$$

where

$$\begin{aligned} D_\alpha &= I_{N-1} \otimes A_1 - \alpha(W \otimes I_{nx}), \\ D_\beta &= I_{N-1} \otimes A_2 - \beta(W \otimes I_{nx}), \\ W &= (\omega_{ij})_{(N-1)\times(N-1)}, \omega_{ij} = \bar{l}_{(i+1)(j+1)} - \bar{l}_{1(j+1)}. \end{aligned}$$

Remark 4 [18]: One has $\omega_i = 1$ for all $i = 1, 2, \ldots, N$, the bipartite synchronization reduces to the traditional synchronization.

Remark 5: As in the work in [18], [19], and [20], by introducing gauge transformation, the bipartite synchronization problem of system (3) with adjacency matrix $\mathcal{A} = (a_{ij})_{N\times N}$ is transformed into the synchronization problem of system (4) with adjacency matrix $\bar{\mathcal{A}} = (|a_{ij}|)_{N\times N}$. Correspondingly, the Laplacian matrix $L = (l_{ij})_{N\times N}$ becomes the Laplacian matrix $\bar{L} = (\bar{l}_{ij})_{N\times N}$, the row sum of the former is not all zero, and the latter is a zero-row sum matrix.

Definition 3 [33]: (Average Impulse Interval). The average impulse sequence $\{t_p\}_{p=1}^{\infty}$ is regarded to not be less than T_a, if there exist a positive integer N_0 and a positive number T_a that satisfies the following conditions:

$$N(t_0, t) \leq N_0 + \frac{t - t_0}{T_a},$$

where $N(t_0, t)$ represents the number of impulsive times in the time period t_0 to t.

Lemma 1 [34]: If the signed graph contains a directed spanning tree, then Laplacian matrix $\bar{L} = \bar{l}_{ij} = (\omega_i l_{ij} \omega_j)_{N\times N}$ has a single zero eigenvalue and the other $N-1$ eigenvalues all lie in the right half-plane.

Lemma 2 [35]: If the signed graph contains a directed spanning tree, then the matrix $W = (\omega_{ij})_{(N-1)\times(N-1)}$ has no zero eigenvalues and all of its eigenvalues have positive real parts.

Lemma 3 [36]: (Halanay Differential Inequality) Suppose there is a non-negative function $V(t), t \in [-\tau, \infty)$, which satisfies the following:

$$\begin{aligned} &\dot{V}(t) \leq -aV(t) + b\bar{V}(t), t \geq t_0, \quad 0 \leq b < a, \\ &\bar{V}(t) \triangleq \sup_{s\in[t-\tau,t]} V(s), \end{aligned}$$

then, $V(t) \leq \bar{V}(t_0)e^{-\gamma(t-t_0)}, t \geq t_0$,
where $\gamma > 0$ and γ is the only solution to equation $\gamma - a + be^{\gamma\tau} = 0$.

III. MAIN RESULTS

In this section, several sufficient conditions for the multi-agent system with signed graph in Section 2 is obtained to achieve bipartite synchronization.

Set the following piecewise function $\sigma : [t_0, +\infty) \to \mathbb{R}^+$ by

$$\sigma(t) = \frac{t_p - t}{t_p - t_{p-1}}, \quad t \in \left[t_{p-1}, t_p\right), p \in \mathbb{N},$$

and $\tilde{\sigma}(t) = 1 - \sigma(t)$. It is easy to see that

$$\begin{aligned} &\sigma(t) \in (0, 1] \text{ for } t \geq t_0, \\ &\sigma(t_p^-) = 0, \quad \sigma(t_p) = \sigma(t_p^+) = 1, \quad p \in \mathbb{N}. \end{aligned}$$

Theorem 1: Under Assumption 1-4, the multi-agent system (2) can achieve bipartite synchronization, if for given scalars $\lambda > \varepsilon > 0$, $\gamma > 1$, there exist matrices $P_i > 0$, $i = 1, 2$, scalars $\delta_1 > 0, \delta_2 > 0$ and $r > 0$, such that the following linear matrix inequalities hold:

$$P_i < rI_{(N-1)nx}, \quad i = 1, 2 \tag{6}$$

$$\begin{bmatrix} \Omega_{i11} & P_i(I_{N-1} \otimes B_1) & P_iD_\beta & P_i(I_{N-1} \otimes B_2) \\ * & -\delta_1 I_{(N-1)nx} & 0 & 0 \\ * & * & \Omega_{i33} & 0 \\ * & * & * & -\delta_2 I_{(N-1)nx} \end{bmatrix} < 0, i = 1, 2 \tag{7}$$

where $\Omega_{i11} = P_iD_\alpha + D_\alpha^T P_i + \frac{P_1 - P_2}{h} + \lambda P_i + \delta_1(I_{N-1} \otimes \Upsilon^T\Upsilon)$ and $\Omega_{i33} = -\varepsilon P_i + \delta_2(I_{N-1} \otimes \Upsilon^T\Upsilon)$.

$$(P_2 - \gamma P_1) + 2\bar{\rho}\theta\lambda_{\max}(P_2) + \bar{\rho}\theta^2\lambda_{\max}(P_2)I_{(N-1)nx} < 0 \tag{8}$$

$$a - \frac{\ln \gamma}{T_a} > 0 \tag{9}$$

where a satisfies $a - \lambda + \varepsilon e^{a\bar{\tau}} = 0$.

Proof: Consider the following Lyapunov function:

$$V(t) = e^T(t)\left(\tilde{\sigma}(t)P_1 + \sigma(t)P_2\right)e(t) \tag{10}$$

From Assumption 1, one obtains:

$$\eta^T(t)\eta(t) - e^T(t)(I_{N-1} \otimes \Upsilon^T\Upsilon)e(t) \leq 0 \tag{11}$$

$$\begin{aligned} &\eta^T(t - \tau(t))\eta(t - \tau(t)) - e^T(t - \tau(t))(I_{N-1} \otimes \Upsilon^T\Upsilon) \\ &\qquad \times e(t - \tau(t)) \leq 0 \end{aligned} \tag{12}$$

where $\Upsilon = diag\{\upsilon_1, \upsilon_2, \ldots \upsilon_{nx}\}$.

When $t \in \left[t_{p-1}, t_p\right)$, the derivative of $V(t)$ along the multi-agent system is expressed as:

$$\dot{V}(t) = 2e^T(t)\left(\tilde{\sigma}(t)P_1 + \sigma(t)P_2\right)\dot{e}(t) - \frac{1}{h}e^T(t)\left(P_2 - P_1\right)e(t) \tag{13}$$

By introducing all $\delta_1 > 0, \delta_2 > 0$, inequalities (11) and (12) into equation (13), it follows that for

$$\begin{aligned} \dot{V}(t) \leq\ & 2e^T(t)\left(\tilde{\sigma}(t)P_1 + \sigma(t)P_2\right)\left(D_\alpha e(t) + (I_{N-1} \otimes B_1)\eta(t)\right. \\ & \left. + D_\beta e(t - \tau(t)) + (I_{N-1} \otimes B_2)\eta(t - \tau(t))\right) \\ & - \frac{1}{h}e^T(t)\left(P_2 - P_1\right)e(t) + \varepsilon V(t - \tau(t)) \\ & - \varepsilon e^T(t - \tau(t))\left(\tilde{\sigma}(t)P_1 + \sigma(t)P_2\right)e(t - \tau(t)) \\ & - \lambda V(t) + \lambda e^T(t)\left(\tilde{\sigma}(t)P_1 + \sigma(t)P_2\right)e(t) \\ & + \delta_1\left(e^T(t)(I_{N-1} \otimes \Upsilon^T\Upsilon)e(t) - \eta^T(t)\eta(t)\right) \\ & + \delta_2\left(e^T(t - \tau(t))\left(I_{N-1} \otimes \Upsilon^T\Upsilon\right)e(t - \tau(t))\right) \\ & - \delta_2\left(\eta^T(t - \tau(t))\eta(t - \tau(t))\right) \\ =\ & \xi^T(t)\left(\tilde{\sigma}(t)\Omega_1 + \sigma(t)\Omega_2\right)\xi(t) - \lambda V(t) + \varepsilon V(t - \tau(t)) \end{aligned} \tag{14}$$

where $\xi(t) = \left[e^T(t)\ \eta^T(t)\ e^T(t - \tau(t))\ \eta^T(t - \tau(t))\right]^T$ and Ω_i is expressed as shown in the equation at the bottom of the page, where $\Omega_{i11} = P_iD_\alpha + D_\alpha^T P_i + \frac{P_1 - P_2}{h} + \lambda P_i + \delta_1(I_{N-1} \otimes \Upsilon^T\Upsilon)$

$$\Omega_{i33} = -\varepsilon P_i + \delta_2(I_{N-1} \otimes \Upsilon^T\Upsilon).$$

According to (7), $\Omega_1 < 0$ and $\Omega_2 < 0$, it follows from (14) that

$$\dot{V}(t) \leq -\lambda V(t) + \varepsilon V(t - \tau(t)), t \in \left[t_{p-1}, t_p\right) \tag{15}$$

By Lemma 3, one has:

$$V(t) \leq \sup_{s \in [t_{p-1} - \bar{\tau}, t_{p-1}]} V(s)e^{-a(t - t_{p-1})}, t \in \left[t_{p-1}, t_p\right) \tag{16}$$

where $a > 0$ and a satisfies $a - \lambda + \varepsilon e^{a\bar{\tau}} = 0$.

When $t = t_p$, the mathematical expectation of $V(t_p)$ is expanded as follows:

$$\begin{aligned} E\left\{V(t_p)\right\} &= E\left\{e^T(t_p)P_2e(t_p)\right\} \\ &= E\left\{\left[(e(t_P^-) + \rho(t_p^-)\varphi(t_p^-)\right]^T\right. \\ &\quad \left. \times P_2\left[(e(t_P^-) + \rho(t_p^-)\varphi(t_P^-)\right]\right\} \\ &= e^T(t_P^-)P_2e(t_P^-) + 2\bar{\rho}e^T(t_p^-)P_2\varphi(t_p^-) \\ &\quad + \bar{\rho}\varphi^T(t_p^-)P_2\varphi(t_p^-). \end{aligned} \tag{17}$$

According to Assumption 2, the following inequalities hold:

$$2e^T(t_p^-)P_2\varphi(t_p^-) \leq 2\lambda_{\max}(P_2)\theta\left\|e^T(t_p^-)\right\|^2 \tag{18}$$

$$\varphi^T(t_p^-)P_2\varphi(t_p^-) \leq \lambda_{\max}(P_2)\theta^2\left\|e^T(t_p^-)\right\|^2 \tag{19}$$

$$\Omega_i = \begin{bmatrix} \Omega_{i11} & P_i(I_{N-1} \otimes B_1) & P_iD_\beta & P_i(I_{N-1} \otimes B_2) \\ * & -\delta_1 I_{(N-1)nx} & 0 & 0 \\ * & * & \Omega_{i33} & 0 \\ * & * & * & -\delta_2 I_{(N-1)nx} \end{bmatrix}, \quad i = 1, 2$$

Therefore,

$$\begin{aligned}E\left\{V(t_p)\right\} &\le e^T(t_p^-)P_2e(t_p^-)+2\bar{\rho}\theta\lambda_{\max}(P_2)\left\|e^T(t_p^-)\right\|^2\\&\quad+\bar{\rho}\theta^2\lambda_{\max}(P_2)\left\|e^T(t_p^-)\right\|^2-\gamma e^T(t_p^-)P_1e(t_p^-)\\&\quad+\gamma e^T(t_p^-)P_1e(t_p^-)\\&=e^T(t_p^-)\left(P_2-\gamma P_1\right)e(t_p^-)\\&\quad+2\bar{\rho}\theta\lambda_{\max}(P_2)\left\|e^T(t_p^-)\right\|^2\\&\quad+\bar{\rho}\theta^2\lambda_{\max}(P_2)\left\|e^T(t_p^-)\right\|^2+\gamma V(t_p^-)\\&=e^T(t_p^-)\left(\left(P_2-\gamma P_1\right)\right.\\&\quad\left.+2\bar{\rho}\theta\lambda_{\max}(P_2)+\bar{\rho}\theta^2\lambda_{\max}(P_2)I_{(N-1)nx}\right)e(t_p^-)\\&\quad+\gamma V(t_p^-)\end{aligned}\tag{20}$$

Then, from inequality (8), it can be known that

$$E\left\{V(t_p)\right\}\le\gamma V(t_p^-).\tag{21}$$

So that, for $t\in\left[t_{p-1},t_p\right)$,

$$\begin{aligned}E\left\{V(t_p)\right\}&\le\bar{V}(t_{p-1})e^{-\alpha(t-t_{p-1})}\\&\le\gamma\bar{V}(t_{p-1}^-)e^{-\alpha(t-t_{p-1})}\\&\le\gamma^2\bar{V}(t_{p-2}^-)e^{-\alpha(t_{p-1}-t_{p-2})}e^{-\alpha(t-t_{p-1})}\\&\le\cdots\\&\le\gamma^{p-1}\bar{V}(t_0)e^{-\alpha(t-t_0)}\\&\le\gamma^{N(t_0,t)}\lambda_{\max}(P_i)\vartheta e^{-\alpha(t-t_0)}.\end{aligned}\tag{22}$$

where $\vartheta=\sup_{s\in[-\bar{\tau},0]}\|e(s)\|^2$.

By Definition 3, the following inequality can be obtained for $t\in\left[t_{p-1},t_p\right)$,

$$\lambda_{\min}(P_i)E\left\{\|e\|^2\right\}\le E\left\{V(t_p)\right\}\le\gamma^{N_0}\lambda_{\max}(P_i)\vartheta e^{-(a-\frac{\ln\gamma}{T_a})(t-t_0)}\tag{23}$$

Then

$$E\left\{\|e\|^2\right\}\le ce^{-(a-\frac{\ln\gamma}{T_a})(t-t_0)},\ c=\frac{\gamma^{N_0}\lambda_{\max}(P_i)\vartheta}{\lambda_{\min}(P_i)}\tag{24}$$

According to the inequality (9), one obtains:

$$\lim_{t\to\infty}E\left\{\|e\|^2\right\}=0\tag{25}$$

Combined with the condition of bipartite synchronization in Definition 2, the multi-agent system with signed graph can achieve bipartite synchronization, and the proof is complete.

Remark 6: Under Assumptions 1-2 of the node function and Assumptions 3-4 of the system topology, by constructing a Lyapunov function and applying Halanay differential inequality in Lemma 3, Theorem 1 provides a new bipartite synchronization criterion for multi-agent systems under time-varying delay and deception attacks. The criterion involves the Kronecker product.

If the delayed node state terms are not included in the multi-agent system, the system (2) becomes

$$\begin{cases}\dot{x}_i(t)=A_1x_i(t)+B_1f(x_i(t))\\-\alpha\sum_{j=1}^{N}\left|g_{ij}\right|\left(x_i(t)-sign(g_{ij})x_j(t)\right)\\-\beta\sum_{j=1}^{N}\left|g_{ij}\right|\left(x_i(t-\tau(t))-sign(g_{ij})x_j(t-\tau(t))\right),\ t\ne t_p,\\\Delta x_i(t_p)=\rho(t_p)k(x_i(t_p^-)),\ p\in\mathbb{N}^+.\end{cases}\tag{26}$$

then the corresponding bipartite synchronization condition is derived by setting $A_2=0,B_2=0$.

Corollary 1: Under Assumptions 1-4, the multi-agent system (26) can achieve bipartite synchronization, if for given scalars $\lambda>\varepsilon>0,\gamma>1$, there exist matrices $P_i>0$, $i=1,2$, scalars $\delta_1>0$ and $r>0$, such that the following linear matrix inequalities hold:

$$P_i<rI_{(N-1)nx},\quad i=1,2\tag{27}$$

$$\begin{bmatrix}\Omega_{i11}&P_i(I_{N-1}\otimes B)&-\beta P_i(W\otimes I_{nx})\\*&-\delta_1I_{(N-1)nx}&0\\*&*&-\varepsilon P_i\end{bmatrix}<0,\quad i=1,2\tag{28}$$

where $\Omega_{i11}=P_iD_\alpha+D_\alpha^TP_i+\frac{P_1-P_2}{h}+\lambda P_i+\delta_1(I_{N-1}\otimes\Upsilon^T\Upsilon)$,

$$\left(P_2-\gamma P_1\right)+2\bar{\rho}\theta\lambda_{\max}(P_2)+\bar{\rho}\theta^2\lambda_{\max}(P_2)I_{(N-1)nx}<0\tag{29}$$

$$a-\frac{\ln\gamma}{T_a}>0\tag{30}$$

where a satisfies $a-\lambda+\varepsilon e^{a\bar{\tau}}=0$.

If the delayed coupling terms are not included in the multi-agent system, the system (2) becomes

$$\begin{cases}\dot{\bar{x}}_i(t)=A_1\bar{x}_i(t)+A_2\bar{x}_i(t-\tau(t))+B_1f(\bar{x}_i(t))\\+B_2f(\bar{x}_i(t-\tau(t)))-\alpha\sum_{j=1}^{N}\bar{l}_{ij}\bar{x}_j(t),\ t\ne t_p\\\Delta\bar{x}_i(t_p)=\rho(t_p)k(\bar{x}_i(t_p^-)),\ p\in\mathbb{N}^+.\end{cases}\tag{31}$$

then the corresponding bipartite synchronization condition is derived by setting $\beta=0$.

Corollary 2: Under Assumptions 1-4, the multi-agent system (31) can achieve bipartite synchronization, if for given scalars $\lambda>\varepsilon>0,\gamma>1$, there exist matrices $P_i>0$, $i=1,2$, scalars $\delta_1>0,\delta_2>0$ and $r>0$, such that the following linear matrix inequalities hold:

$$P_i<rI_{(N-1)nx},\quad i=1,2\tag{32}$$

(33), as shown at the bottom of the next page, where $\Omega_{i11}=P_iD_\alpha+D_\alpha^TP_i+\frac{P_1-P_2}{h}+\lambda P_i+\delta_1(I_{N-1}\otimes\Upsilon^T\Upsilon)$ and $\Omega_{i33}=-\varepsilon P_i+\delta_2(I_{N-1}\otimes\Upsilon^T\Upsilon)$

$$\left(P_2-\gamma P_1\right)+2\bar{\rho}\theta\lambda_{\max}(P_2)+\bar{\rho}\theta^2\lambda_{\max}(P_2)I_{(N-1)nx}<0\tag{34}$$

$$a-\frac{\ln\gamma}{T_a}>0\tag{35}$$

where a satisfies $a-\lambda+\varepsilon e^{a\bar{\tau}}=0$.

If the deception attacks are not considered in the multi-agent system, the system (2) becomes

$$\begin{cases} \dot{x}_i(t) = A_1 x_i(t) + A_2 x_i(t-\tau(t)) + B_1 f(x_i(t)) \\ + B_2 f(x_i(t-\tau(t))) - \alpha \sum_{j=1}^{N} \left|g_{ij}\right| (x_i(t) - sign(g_{ij}) x_j(t)) \\ -\beta \sum_{j=1}^{N} \left|g_{ij}\right| (x_i(t-\tau(t)) - sign(g_{ij}) x_j(t-\tau(t))), t \neq t_p, \\ \Delta x_i(t_p) = 0, p \in \mathbb{N}^+. \end{cases} \tag{36}$$

Note $\rho(t_p) = 0$, that is, there is no deception attack in the system (2). Then, the following corollary can be drawn:

Corollary 3: Under Assumptions 1-4, the multi-agent system (37) can achieve bipartite synchronization, if for given scalars $\lambda > \varepsilon > 0$, $\gamma > 1$, there exist matrices $P_i > 0$, $i = 1, 2$, scalars $\delta_1 > 0, \delta_2 > 0$ and $r > 0$, such that the following linear matrix inequalities hold:

$$P_i < rI_{(N-1)nx}, i = 1, 2 \tag{37}$$

(38), as shown at the bottom of the page, where $\Omega_{i11} = P_i D_\alpha + D_\alpha^T P_i + \frac{P_1 - P_2}{h} + \lambda P_i + \delta_1 (I_{N-1} \otimes \Upsilon^T \Upsilon)$ and

$$\begin{aligned} \Omega_{i33} = & -\varepsilon P_i + \delta_2 (I_{N-1} \otimes \Upsilon^T \Upsilon). \\ & \times (P_2 - \gamma P_1) + 2\bar{\rho}\theta \lambda_{\max}(P_2) \\ & + \bar{\rho}\theta^2 \lambda_{\max}(P_2) I_{(N-1)nx} < 0 \end{aligned} \tag{39}$$

$$a - \frac{\ln \gamma}{T_a} > 0 \tag{40}$$

where a satisfies $a - \lambda + \varepsilon e^{a\bar{\tau}} = 0$.

IV. NUMERICAL SIMULATION

This section presents two numerical examples to demonstrate the validity of our results in Section 3, both of which employ a chaotic system to describe the dynamic behavior of isolated node in system (2).

Example 1: Consider a multi-agent system with signed graph of seven nodes, whose topology is the same as in [37], shown in Figure 1. Each chaotic agent can be regarded as a node in the system. The dynamic behavior of each individual agent is described by (2) with:

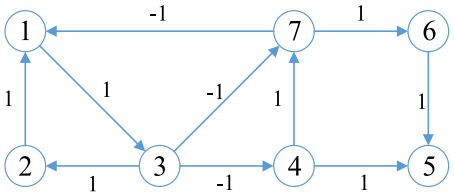

FIGURE 1. Multi-agent system composed of seven nodes.

$$\begin{aligned} A1 = A2 = & \text{diag}([-1.2, -1.2, -1.2]), \\ B1 = B2 = & \begin{bmatrix} 1.16 & -1.5 & -1.5 \\ -1.5 & 1.16 & -2 \\ -1.2 & 2 & 1.16 \end{bmatrix}, \\ f(x_i(t)) = & \begin{bmatrix} \tanh(x_{i1}(t)) \\ \tanh(x_{i2}(t)) \\ \tanh(x_{i3}(t)) \end{bmatrix}, \\ \alpha = 7, \beta = 0.8, \bar{\rho} = 0.1 & \text{ and } \bar{\tau} = 0.3. \end{aligned}$$

It can be verified that $|f_m(x) - f_m(y)| \leq |x - y|, \forall x, y \in \mathbb{R}$ with $m = 1, 2, 3$.

From the above topology, the entire system is divided into two clusters, $\mathcal{N}_1 = \{1, 2, 3\}$ and $\mathcal{N}_2 = \{4, 5, 6, 7\}$. The structure of the system is balanced and contains a directed spanning tree.

Let λ=2, ε=1 and $\bar{\tau} = 0.3$, then $a = 0.7483$ is the root of the equation $a - \lambda + \varepsilon e^{a\bar{\tau}} = 0$. Set $\psi(x_i(t)) = [0.3x_{i1}(t), -0.3\sin(x_{i2}(t)), 0.3\tanh(x_{i3}(t))]^T$, then $\|\psi(z_1) - \psi(z_2)\| \leq \theta \|z_1 - z_2\|, \forall z_1, z_2 \in \mathbb{R}^3$ with θ=0.3. Meanwhile, let $T_a = 0.5$ and $\gamma = 1.35$ such that $a - \frac{\ln \gamma}{T_a} > 0$ can be hold. Then feasible results are then solved by using linear matrix inequality technology. In the simulation, the impulse interval is taken as 0.5s.

Figure 2 depicts the trajectories of $x_i (i = 1, 2, \ldots 7)$ and the deception attacks occurrence at impulse instants. It can be seen from the figure that, at the impulse instants when the deception attacks really occur, even though the system states will be affected to make a jump, the trajectory of the system states will still maintain bipartite synchronization.

$$\begin{bmatrix} \Omega_{i11} & P_i(I_{N-1} \otimes B_1) & P_i(I_{N-1} \otimes A_2) & P_i(I_{N-1} \otimes B_2) \\ * & -\delta_1 I_{(N-1)nx} & 0 & 0 \\ * & * & \Omega_{i33} & 0 \\ * & * & * & -\delta_2 I_{(N-1)nx} \end{bmatrix} < 0, \quad i = 1, 2 \tag{33}$$

$$\begin{bmatrix} \Omega_{i11} & P_i(I_{N-1} \otimes B_1) & P_i(I_{N-1} \otimes A_2) & P_i(I_{N-1} \otimes B_2) \\ * & -\delta_1 I_{(N-1)nx} & 0 & 0 \\ * & * & \Omega_{i33} & 0 \\ * & * & * & -\delta_2 I_{(N-1)nx} \end{bmatrix} < 0, \quad i = 1, 2 \tag{38}$$

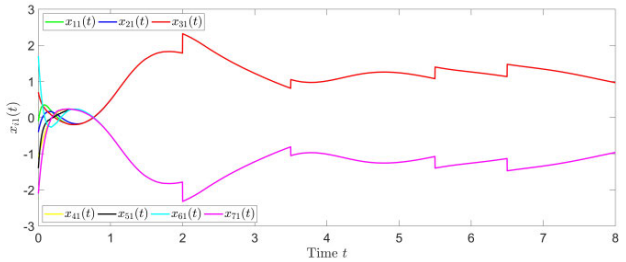

(a) State trajectory of $x_{i1}(t)(i = 1, 2, \ldots, 7)$

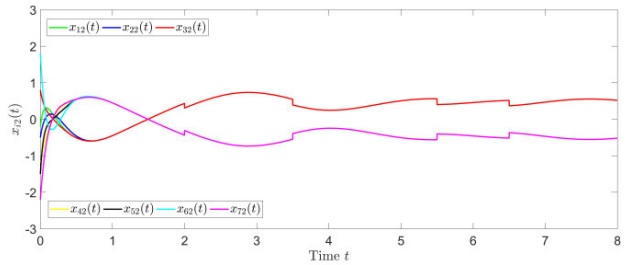

(b) State trajectory of $x_{i2}(t)(i = 1, 2, \ldots, 7)$

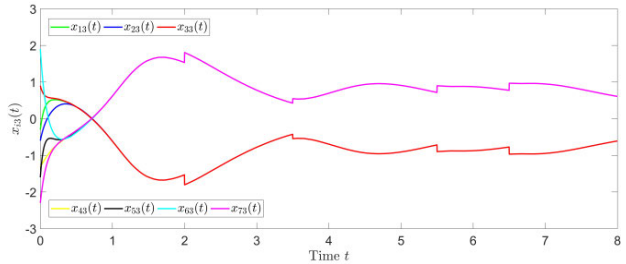

(c) State trajectory of $x_{i3}(t)(i = 1, 2, \ldots, 7)$

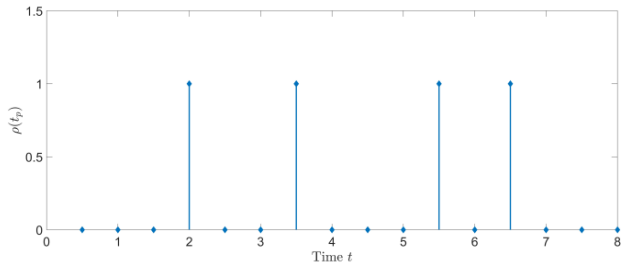

(d) Deception attacks occurrence at impulse instants

FIGURE 2. State trajectories of $x_i(t)(i = 1, 2, \ldots, 7)$ and the deception attacks occurrence at impulse instants.

These simulation results demonstrate the effectiveness of the proposed bipartite synchronization approach.

Example 2: Consider a multi-agent system with signed graph composed by nine nodes, whose topology is the same as in [19] and [38] and shown in Figure 3. Each chaotic agent can be regarded as a node, which is described by equation (2) with:

$$A1 = \begin{bmatrix} -1 & 0 \\ 0 & -1 \end{bmatrix}, \quad A2 = \begin{bmatrix} -0.1 & 0 \\ 0 & -0.1 \end{bmatrix},$$

$$B1 = \begin{bmatrix} 1+\frac{\pi}{4} & 20 \\ 0.1 & 1+\frac{\pi}{4} \end{bmatrix}, \quad B2 = \begin{bmatrix} -\frac{1.3\pi\sqrt{2}}{4} & 0.1 \\ 0.1 & -\frac{1.3\pi\sqrt{2}}{4} \end{bmatrix},$$

$$f(x_i(t)) = \begin{bmatrix} 0.5(|x_{i1}(t)+1| - |x_{i1}(t)-1|) \\ 0.5(|x_{i2}(t)+1| - |x_{i2}(t)-1|) \end{bmatrix}, \quad \tau(t) = 1.$$

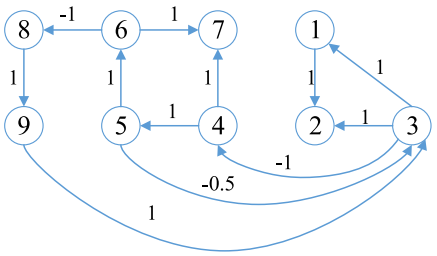

FIGURE 3. Multi-agent system composed of nine nodes.

It can be verified that $|f_1(x) - f_1(y)| \leq \nu_1 |x - y|$, $\forall x, y \in \mathbb{R}$ with $\nu_1 = 1$.

It can be seen from the above topology diagram that the structure of the system is balanced and the signed graph contains a directed spanning tree. The system can be divided into two clusters, which are $\mathcal{N}_1 = \{1, 2, 3, 8, 9\}$ and $\mathcal{N}_2 = \{4, 5, 6, 7\}$.

Assume $\alpha = 15, \beta = 1, \psi(x_i(t)) = [0.3x_{i1}(t), -0.3\sin(x_{i2}(t))]^T$ and parameters θ, $\bar{\rho}$ are same as those in example 1.

Let $\lambda = 1$, $\varepsilon = 0.5$ and $\bar{\tau} = 1$, then $a = 0.3149$ is the root of the equation $a - \lambda + \varepsilon e^{a\bar{\tau}} = 0$. Meanwhile, in order to meet the condition $a - \frac{\ln\gamma}{T_a} > 0$, it is set that $T_a = 1$ and $\gamma = 1.3610$. Feasible results are then obtained by solving the linear matrix inequalities in Theorem 1. In the simulation, the impulse interval is taken as 1s, that is $t_p - t_{p-1} = 1s$.

Figure 4 shows the trajectories of $x_i(i = 1, 2, \ldots 9)$, and the deception attacks occurrence at impulse instants are also depicted. It is clear that the trajectory of the system states will still keep bipartite synchronous, even if the system states will be affected to jump at the impulse instants with deception attacks. These simulation results further illustrate the effectiveness of the proposed bipartite synchronization approach.

V. APPLICATION TO SPEECH COMMUNICATION

Multi-agent systems usually need to keep necessary communication, such as speech, video, text chat and so on, but the security of communication must be guaranteed. Based on the synchronization results of Example 1 obtained in Section 4, a new chaotic speech secure communication system is constructed to verify the feasibility of the proposed theoretical method.

A. SPEECH SECURE COMMUNICATION

Usually, duplex speech communication can be performed between agents. For simplicity, the simplex communication in which the agent i sends the encrypted speech signals to the agent j is taken as an example for analysis. As shown in Figure 5, a typical speech secure communication system consists of two parts, the sender and receiver. The sender of agent i encrypts a section of speech signals to produce signals similar to white noise by using the chaotic signals which are generated by node i in the multi-agent system (2). Then

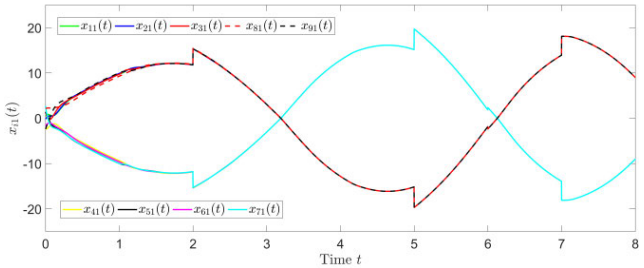

(a) State trajectory of $x_{i1}(t)(i=1,2,\ldots,9)$

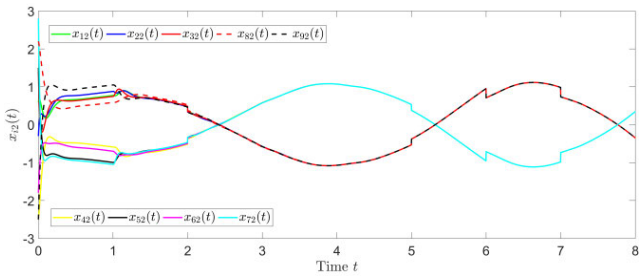

(b) State trajectory of $x_{i2}(t)(i=1,2,\ldots,9)$

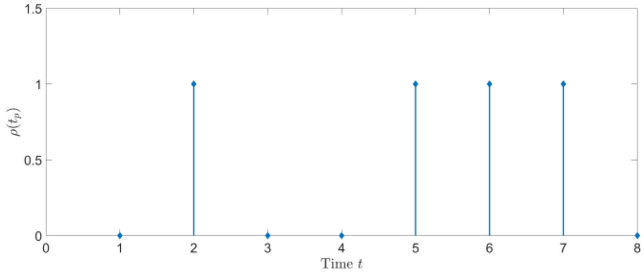

(c) Deception attacks occurrence at impulse instants

FIGURE 4. State trajectories of $x_i(t)(i = 1, 2, \ldots, 9)$ and the deception attacks occurrence at impulse instants.

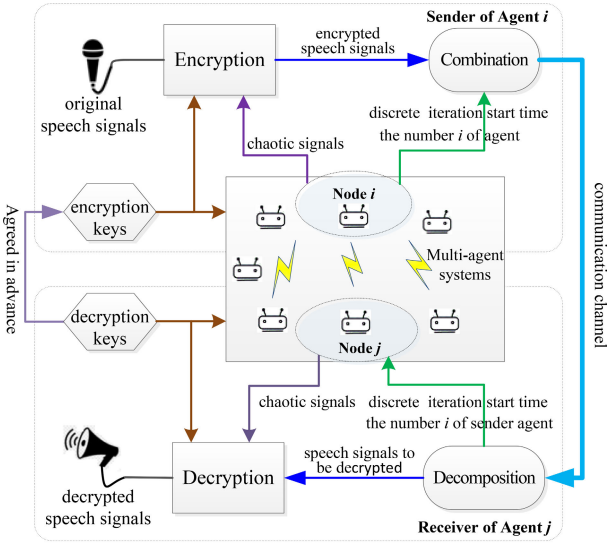

FIGURE 5. Block diagram of speech secure communication system based on bipartite synchronization.

the encrypted speech signals, the discrete iteration start time (N_l_k) and the number i of agent are combined into a data packet to send. Accordingly, after receiving the data packet, the receiver of agent j decomposes it into the corresponding speech signals to be decrypted, the discrete iteration start time $(\bar{N}_l\_k)$ and the number i of sender agent. The multi-agent systems with signed digraph, time-varying delay and deception attacks can realize bipartite synchronization to recover the original speech signals under the guarantee of Theorem 1, in which the chaotic signals generated by node i are used for speech encryption, while signals generated by node j are used for speech decryption. Furthermore, if and only if the encryption and decryption keys are completely consistent, it can be ensured that the sender of agent i and the receiver of agent j can produce the same or opposite key streams to recover the original speech signals. For simplicity, it is assumed that the encryption keys and the decryption keys are agreed in advance by both the sender of agent i and the receiver of agent j. The sender and receiver can be attached to the agent. In addition, the channel used for speech communication is a separate channel, independent of the topology of the multi-agent system with signed graph.

The workflow of chaotic speech secure communication between agent i and agent j is described as follows.

Step 1: A section of original speech signals to be sent by agent i is prepared. There are two kinds of voice, one is to record directly and send in real time, and the other is to read data directly from the recording file. Without losing generality, a direct recording is performed with the frequency of 8000Hz, and the resulting original speech signal is expressed as $m(t)$.

Step 2: Given the parameter matrices $(A1, B1, A2, B2)$, iteration step size (ΔT) and initial values $((x_{11}(0), x_{12}(0), x_{13}(0))^T, (x_{21}(0), x_{22}(0), x_{23}(0))^T, (x_{31}(0), x_{32}(0), x_{33}(0))^T, (x_{41}(0), x_{42}(0), x_{43}(0))^T, (x_{51}(0), x_{52}(0), x_{53}(0))^T, (x_{61}(0), x_{62}(0), x_{63}(0))^T, (x_{71}(0), x_{72}(0), x_{73}(0))^T)$ of multi-agent system (2), three chaotic state sequences of each node are obtained after discretization and iteration operations, expressed as $x_{mn} = \{x_{mn}(0), \ldots, x_{mn}(k), \ldots\}$, $m = 1, 2, \ldots, 7, n = 1, 2, 3$, where the chaotic state sequences generated by node i are used as encryption key streams.

Given the initial encryption value (C_temp), according to Algorithm 1, at the sending end of agent i, the original speech signal is encrypted by using the generated chaotic state sequences x_{in} $(n= 1, 2, 3)$, that is, the encrypted speech signals are obtained.

Step 3: The encrypted speech signal $C(t)$, the discrete iteration start time (N_1_k, N_2_k, N_3_k) and the number i of agent sender are combined into a data packet for transmission. Immediately, agent i sends the data packet to agent j. For simplicity, the one-encryption and one-transmission mode is adopted here. However, it is recommended to use segment-encryption and segment-transmission mode for long time speech signals.

After receiving the data packet, the receiver of agent j decomposes it into the corresponding speech signal to be decrypted $\bar{C}(t)$, discrete iteration start time $(\bar{N}_1\_k, \bar{N}_2\_k, \bar{N}_3\_k)$ and the number i of agent sender, which is transmitted through the exclusive communication channel.

Algorithm 1 Speech Encryption

Initialization:

Set $L \leftarrow length(m(t))$; $N_1\_k \leftarrow 3000 + i$; $N_2\_k \leftarrow 3007 + i$; $N_3\_k \leftarrow 3011 + i$;

for $k = 1 : \left\lceil L/3 \right\rceil$

$tmp1 = 10 \wedge (9 + mod(floor\ (C\_temp * 10 \wedge 15)\ , 8))$;

$tmp2 = dec2bin\ (mod(floor\ (C\_temp * 10 \wedge 15)\ , 8), 3)$;

$N_1\_k = N_1\_k + 1 + mod(floor\ (C\_temp * tmp1)\ , 3)$;

$N_2\_k = N_2\_k + 1 + mod(floor\ (C\_temp * tmp1)\ , 7)$;

$N_3\_k = N_3\_k + 1 + mod(floor\ (C\_temp * tmp1)\ , 11)$;

$tp21 = (-1) \wedge bin2dec\ (tmp2(1))$;

$tp22 = (-1) \wedge bin2dec\ (tmp2(2))$;

$tp23 = (-1) \wedge bin2dec\ (tmp2(3))$;

if $(mod\ (L, 3) == 2\ \&\&\ p == \left\lceil L/3 \right\rceil) \,||\, (mod\ (L, 3) == 1\ \&\&\ k \geq \left\lceil L/3 \right\rceil - 1)$

$X(k) = mod\ (tp21 * x_{i1}\ (N_1\_k) + tp22 * x_{i2}\ (N_1\_k) + tp23 * x_{i3}\ (N_1\_k)\ , 1)$;

$Y(k) = mod\ (tp21 * x_{i1}\ (N_2\_k) + tp22 * x_{i2}\ (N_2\_k) + tp23 * x_{i3}\ (N_2\_k)\ , 1)$;

$C(k) = mod\ (m\ (k) + 0.5 + 2 * X\ (k) + C\_temp, 1) - 0.5$;

$C\left(\left\lceil L/3 \right\rceil + k\right) = mod\left(m\left(\left\lceil L/3 \right\rceil + k\right) + 0.5 + 3 * Y\ (k) - C\_temp, 1\right) - 0.5$;

$C\_temp = mod\left(C\ (k) + C\left(\left\lceil L/3 \right\rceil + k\right) + C\_temp + X\ (k) + Y(k), 1\right)$;

else

$X(k) = mod\ (tp21 * x_{i1}\ (N_1\_k) + tp22 * x_{i2}\ (N_1\_k) + tp23 * x_{i3}\ (N_1\_k)\ , 1)$;

$Y(k) = mod\ (tp21 * x_{i1}\ (N_2\_k) + tp22 * x_{i2}\ (N_2\_k) + tp23 * x_{i3}\ (N_2\_k)\ , 1)$;

$Z(k) = mod\ (tp21 * x_{i1}\ (N_3\_k) + tp22 * x_{i2}\ (N_3\_k) + tp23 * x_{i3}\ (N_3\_k)\ , 1)$;

$C(k) = mod\ (m\ (k) + 0.5 + 2 * X\ (k) + C\_temp, 1) - 0.5$;

$C\left(\left\lceil L/3 \right\rceil + k\right) = mod\left(m\left(\left\lceil L/3 \right\rceil + k\right) + 0.5 + 3 * Y\ (k) - C\_temp, 1\right) - 0.5$;

$C\left(2 * \left\lceil L/3 \right\rceil + k\right) = mod\left(m\left(2 * \left\lceil L/3 \right\rceil + k\right) + 0.5 - 3 * Z\ (k) + C\_temp, 1\right) - 0.5$;

$C\_temp = mod\left(C\ (k) + C\left(\left\lceil L/3 \right\rceil + k\right) + C\left(2 * \left\lceil L/3 \right\rceil + k\right) + C\_temp + X\ (k) + Y\ (k) + Z\ (k)\ , 1\right)$;

end

end

Step 4: Given the initial value of decryption (P_temp), according to Algorithm 2, at the receiving end of agent j, the encrypted speech signals are decrypted by using the generated chaotic state sequences x_{jn} $(n = 1, 2, 3)$, that is, the original speech signals are recovered.

Remark 7. Algorithms 1 and 2 are suitable for the point-to-point speech communication between multiple agents, using the chaotic signals generated by the point-to-point communication agent itself. These algorithms adopt the parallel encryption/decryption methods, that is, the speech signals are divided into several segments and encrypted/decrypted at the same time, so the encryption/decryption speed is greatly improved. In addition, the chaotic key streams $(X\ (p)\ /\bar{X}\ (q)\ ,\ Y\ (p)\ /\bar{Y}(q)\ and\ Z(p)/\bar{Z}\ (q))$ generated by the multi-agent system with signed digraph are random, which ensures the security of encryption/decryption to a certain extent. The most important is to decide what kind of calculation (1 out of 8) the algorithm performs to generate key streams and where to start extracting chaotic signal, and these operations are not only related to the former key streams

Algorithm 2 Speech Decryption

Initialization:

Set $L \leftarrow length(\bar{C}(t))$;$\bar{N}_1\_k \leftarrow 3000 + i$; $\bar{N}_2\_k \leftarrow 3007 + i$; $\bar{N}_3\_k \leftarrow 3011 + i$;

for $s = 1 : \left\lceil L/3 \right\rceil$

$tmp1 = 10 \wedge (9 + mod(floor\ (P\_temp * 10 \wedge 15)\ , 8))$;

$tmp2 = dec2bin\ (mod(floor\ (P\_temp * 10 \wedge 15)\ , 8), 3)$;

$\bar{N}_1\_k = \bar{N}_1\_k + 1 + mod(floor\ (P\_temp * tmp1)\ , 3)$;

$\bar{N}_2\_k = \bar{N}_2\_k + 1 + mod(floor\ (P\_temp * tmp1)\ , 7)$;

$\bar{N}_3\_k = \bar{N}_3\_k + 1 + mod(floor\ (P\_temp * tmp1)\ , 11)$;

if (i <4 && j >3) || (j <4 && i >3)

$tp21 = (-1) \wedge (bin2dec\ (tmp2\ (1)) + 1)$;

$tp22 = (-1) \wedge (bin2dec\ (tmp2\ (2)) + 1)$;

$tp23 = (-1) \wedge (bin2dec\ (tmp2\ (3)) + 1)$;

else

$tp21 = (-1) \wedge bin2dec\ (tmp2\ (1))$;

$tp22 = (-1) \wedge bin2dec\ (tmp2\ (2))$;

$tp23 = (-1) \wedge bin2dec\ (tmp2\ (3))$;

end

if $(mod\ (L, 3) == 2\ \&\&\ q == \left\lceil L/3 \right\rceil) \,||\, (mod\ (L, 3) == 1\ \&\&\ s \geq \left\lceil L/3 \right\rceil - 1)$

$\bar{X}(s) = mod\left(tp21 * x_{j1}\left(\bar{N}_1\_k\right) + tp22 * x_{j2}\left(\bar{N}_1\_k\right) + tp23 * x_{j3}\left(\bar{N}_1\_k\right), 1\right)$;

$\bar{Y}(s) = mod\left(tp21 * x_{j1}\left(\bar{N}_2\_k\right) + tp22 * x_{j2}\left(\bar{N}_2\_k\right) + tp23 * x_{j3}\left(\bar{N}_2\_k\right), 1\right)$;

$P(s) = mod\left(\bar{C}\ (s) + 0.5 - 2 * \bar{X}(s) - P\_temp, 1\right) - 0.5$;

$P\left(\left\lceil L/3 \right\rceil + s\right) = mod\left(\bar{C}\left(\left\lceil L/3 \right\rceil + s\right) + 0.5 - 3 * \bar{Y}(s) + P\_temp, 1\right) - 0.5$;

$P\_temp = mod\left(\bar{C}\ (s) + \bar{C}\left(\left\lceil L/3 \right\rceil + s\right) + P\_temp + \bar{X}\ (s) + \bar{Y}\ (s)\ , 1\right)$;

else

$\bar{X}\ (s) = mod\left(tp21 * x_{j1}\left(\bar{N}_1\_k\right) + tp22 * x_{j2}\left(\bar{N}_1\_k\right) + tp23 * x_{j3}\left(\bar{N}_1\_k\right), 1\right)$;

$\bar{Y}\ (s) = mod\left(tp21 * x_{j1}\left(\bar{N}_2\_k\right) + tp22 * x_{j2}\left(\bar{N}_2\_k\right) + tp23 * x_{j3}\left(\bar{N}_2\_k\right), 1\right)$;

$\bar{Z}\ (s) = mod\left(tp21 * x_{j1}\left(\bar{N}_3\_k\right) + tp22 * x_{j2}\left(\bar{N}_3\_k\right) + tp23 * x_{j3}\left(\bar{N}_3\_k\right), 1\right)$;

$P(s) = mod\left(\bar{C}\ (s) + 0.5 - 2 * \bar{X}(s) - P\_temp, 1\right) - 0.5$;

$P\left(\left\lceil L/3 \right\rceil + s\right) = mod\left(\bar{C}\left(\left\lceil L/3 \right\rceil + s\right) + 0.5 - 3 * \bar{Y}(s) + P\_temp, 1\right) - 0.5$;

$P\left(2 * \left\lceil L/3 \right\rceil + s\right) = mod\left(\bar{C}\left(2 * \left\lceil L/3 \right\rceil + s\right) + 0.5 + 3 * \bar{Z}(s) - P\_temp, 1\right) - 0.5$;

$P\_temp = mod\left(\bar{C}\ (s) + \bar{C}\left(\left\lceil L/3 \right\rceil + s\right) + \bar{C}\left(2 * \left\lceil L/3 \right\rceil + s\right) + P\_temp + \bar{X}(s) + \bar{Y}\ (s) + \bar{Z}\ (s)\ , 1\right)$;

end

end

but also dependent on the former cipher signals, so as to resist various attacks.

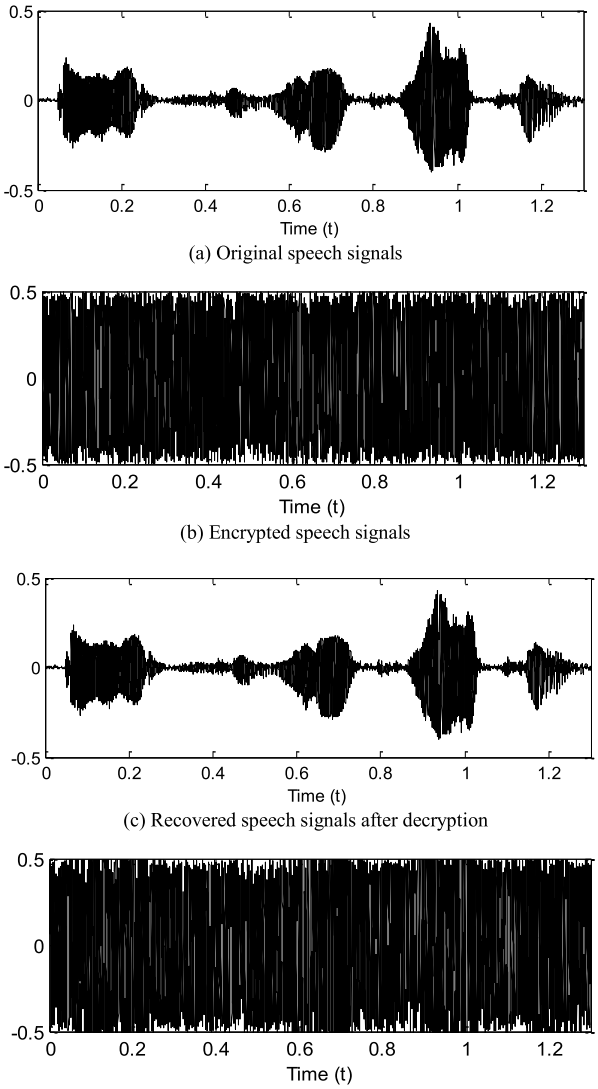

(a) Original speech signals

(b) Encrypted speech signals

(c) Recovered speech signals after decryption

(d) Comparison signals between encrypted and decrypted speech signals

FIGURE 6. Results of speech encryption and decryption.

B. TEST RESULTS AND PERFORMANCE ANALYSIS

Taking Agent 1 sending encrypted speech signals to Agent 5 as an example, this section gives the system test results and performance analysis to prove the effectiveness of the speech secure communication based on the proposed bipartite synchronization method. In this test, the initial encryption/decryption values C_temp/P_temp are all assigned as 0.12345. A section of recording signals to be encrypted is the voice of "speech encryption", as shown in Figure 6(a). The encryption algorithm shown in Algorithm 1 is used to produce encrypted speech signals, as shown in Figure 6(b). It can be seen that the encrypted speech signals are noise without any trace of original information. For simplicity, here Agent 5 used in the speech communication are homogeneous, that is, the parameters of the dynamic system are consistent ($A1 = \bar{A}1, A2 = \bar{A}2, B1 = \bar{B}1, B2 = \bar{B}2$). For decryption, the keys

$$\left(\bar{A}1 = \bar{A}2 = \begin{bmatrix} -1.2 & 0 & 0 \\ 0 & -1.2 & 0 \\ 0 & 0 & -1.2 \end{bmatrix}, \right.$$
$$\bar{B}1 = \bar{B}2 = \begin{bmatrix} 1.16 & -1.5 & -1.5 \\ -1.5 & 1.16 & -2 \\ -1.2 & 2 & 1.16 \end{bmatrix},$$
$$\left.\bar{\Delta T} = 0.002, P\_temp = 0.12345\right)$$

are consistent with the encryption keys which are agreed in advance, and the discrete iteration start time of decryption node $(\bar{N}_1\_k = 3000, \bar{N}_2\_k = 3007, \bar{N}_3\_k = 3011)$ is also consistent with Agent 1. The speech signals recovered after decryption are shown in Figure 6(c), from which it is obvious that the recovered speech signals are the same as the original speech signals. That is to say, Agent 5 can perfectly hear the original speech, while the eavesdropper can only hear a burst of noise during transmission. The Comparison signals between encrypted and decrypted speech signals are depicted in Figure 6(d).

An ideal secure communication must have good performance and enough robustness to resist different types of security attacks. The security analysis presented in this paper includes spectrogram, histogram, key space, key sensitivity and real-time, which are detailed as follows.

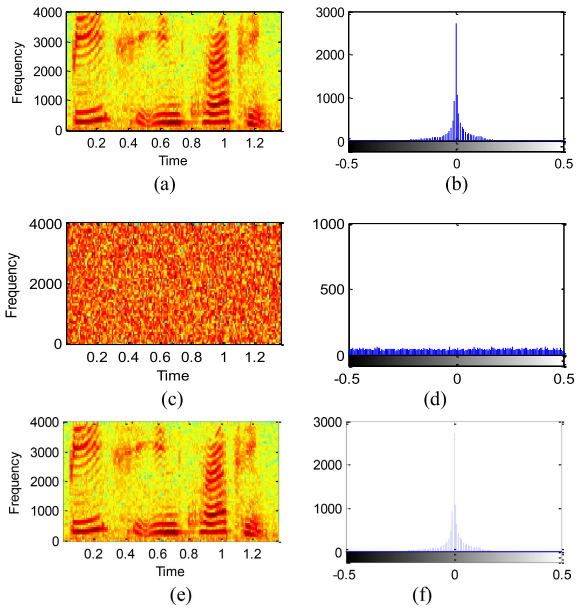

FIGURE 7. Spectrogram and histogram of original speech signals, encrypted speech signals and decrypted speech signals
(a)-(b) Spectrogram and histogram of original speech signals;
(c)-(d) Spectrogram and histogram of encrypted speech signals;
(e)-(f) Spectrogram and histogram of decrypted speech signals.

1) SPECTROGRAM AND HISTOGRAM ANALYSIS

Fig. 7(a) and (b) depict the spectrogram and histogram of the original speech signals whose time domain waveform

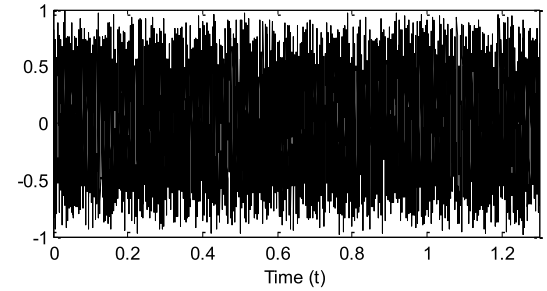

(a) $A1 = \begin{bmatrix} -1.20000000000001 & 0 & 0 \\ 0 & -1.2 & 0 \\ 0 & 0 & -1.2 \end{bmatrix}$

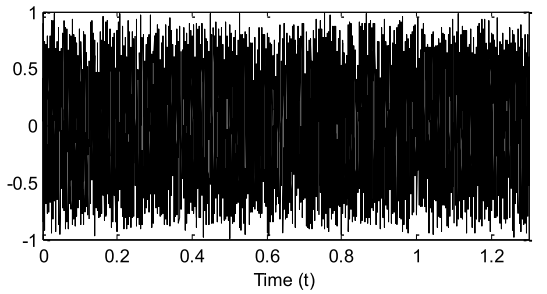

(b) $B1 = \begin{bmatrix} 1.16000000000001 & -1.5 & -1.5 \\ -1.5 & 1.16 & -2 \\ -1.2 & 2 & 1.16 \end{bmatrix}$

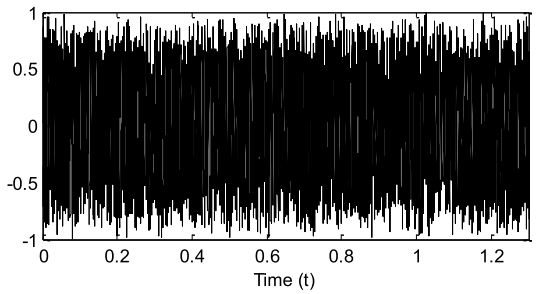

(c) $B1 = \begin{bmatrix} 1.16 & -1.5 & -1.5 \\ -1.5 & 1.16 & -2 \\ -1.2 & 2.00000000000001 & 1.16 \end{bmatrix}$

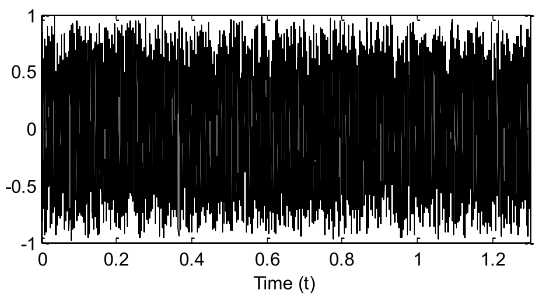

(d) $C\_temp = 0.12345000000001$

FIGURE 8. The errors between the encrypted speech signals generated by the slightly changed encryption keys and the former encrypted speech signals.

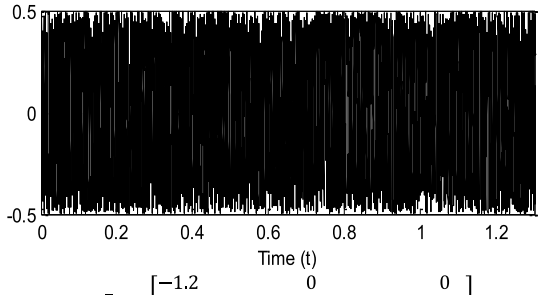

(a) $\bar{A}1 = \begin{bmatrix} -1.2 & 0 & 0 \\ 0 & -1.20000000000001 & 0 \\ 0 & 0 & -1.2 \end{bmatrix}$

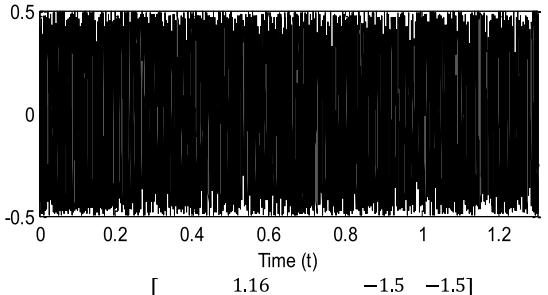

(b) $\bar{B}1 = \begin{bmatrix} 1.16 & -1.5 & -1.5 \\ -1.50000000000001 & 1.16 & -2 \\ -1.2 & 2 & 1.16 \end{bmatrix}$

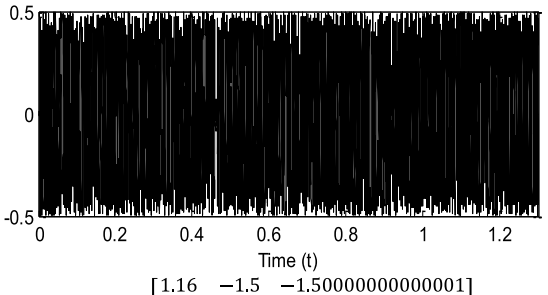

(c) $\bar{B}1 = \begin{bmatrix} 1.16 & -1.5 & -1.50000000000001 \\ -1.5 & 1.16 & -2 \\ -1.2 & 2 & 1.16 \end{bmatrix}$

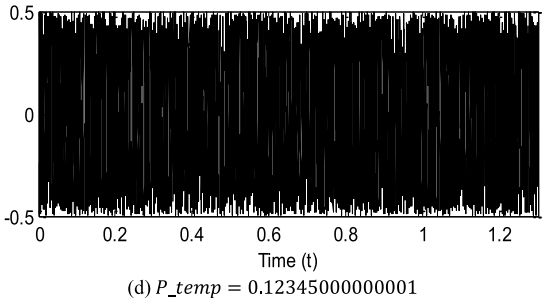

(d) $P\_temp = 0.12345000000001$

FIGURE 9. Decrypted speech signals obtained by using slightly changed decryption keys.

is shown in Figure 6(a). Figure 7(c) and (d) show the spectrogram and histogram of the encrypted speech signals as shown in Figure 6(b). It can be seen that the spectrogram (energy distribution) and histogram (signal value distribution) of the encrypted speech signals are uniform distributed, which are completely different from those of original speech signals, and can well protect the speech information against statistical analysis. In addition, Figure 7(e) and (f) present the spectrogram and histogram of the recovered speech signals after decryption, which are the same as those of the original speech signals.

2) KEY SPACE ANALYSIS

In the proposed algorithm, the keys include the parameter matrices (**A1**, **A2**, **B1**, **B2**) of the multi-agent system with signed digraph shown in (2), the iteration step size $\mathbf{\Delta T}$,

and the encrypted initial value ***C_temp***. It is worth noting that the initial values of multi-agent system with signed graph have no effect on the recovery of original speech signals at receiver. If the calculation accuracy of 64 bit double precision number is $\mathbf{10^{-14}}$, its key space can up to $\mathbf{10^{14\times 18}\times 1000\times 10^{14}=10^{266+3}=10^{269}}$, which is large enough and has sufficient security to resist exhaustive attacks.

3) KEY SENSITIVITY ANALYSIS

An effective encryption algorithm should be sensitive to the keys. On the one hand, even a small change in the encryption keys will lead to a huge difference between the encrypted speech signals. On the other hand, the small difference between the encryption and the decryption keys will fail to recover the original speech signals.

In order to test the sensitivity of encryption keys, only a single encryption key is slightly changed each time. During the test, encryption keys are slightly changed as follows,

$$A1=\begin{bmatrix}-1.2+\omega & 0 & 0\\ 0 & -1.2 & 0\\ 0 & 0 & -1.2\end{bmatrix},$$
$$B1=\begin{bmatrix}1.16+\omega & -1.5 & -1.5\\ -1.5 & 1.16 & -2\\ -1.2 & 2 & 1.16\end{bmatrix},$$
$$B1=\begin{bmatrix}1.16 & -1.5 & -1.5\\ -1.5 & 1.16 & -2\\ -1.2 & 2+\omega & 1.16\end{bmatrix},$$

and C_temp=0.12345+ω, where $\omega = 0.00000000000001$. The error speech signals are respectively shown in Figure 8, which are obtained by comparing the encrypted speech signals using slightly changed encryption keys with the former signals shown in Figure 6(b). It is obvious that ''a millimeter miss'' of the encryption key will lead to ''a thousand miles'' between encrypted speech signals. Therefore, the proposed Algorithm 1 is sensitive to the encryption keys.

In order to test the sensitivity between encryption and decryption keys, a group of decryption keys is similarly selected with tiny modification to decrypt signals in Figure 6(b), such as

$$\bar{A}\mathbf{1}=\begin{bmatrix}\mathbf{-1.2} & \mathbf{0} & \mathbf{0}\\ \mathbf{0} & \mathbf{-1.2}+\bar{\omega} & \mathbf{0}\\ \mathbf{0} & \mathbf{0} & \mathbf{-1.2}\end{bmatrix},$$
$$\bar{B}\mathbf{1}=\begin{bmatrix}\mathbf{1.16} & \mathbf{-1.5} & \mathbf{-1.5}\\ \mathbf{-1.5}+\bar{\omega} & \mathbf{1.16} & \mathbf{-2}\\ \mathbf{-1.2} & \mathbf{2} & \mathbf{1.16}\end{bmatrix},$$
$$\bar{B}\mathbf{1}=\begin{bmatrix}\mathbf{1.16} & \mathbf{-1.5} & \mathbf{-1.5}+\bar{\omega}\\ \mathbf{-1.5} & \mathbf{1.16} & \mathbf{-2}\\ \mathbf{-1.2} & \mathbf{2} & \mathbf{1.16}\end{bmatrix}$$

and $\mathbf{P\_temp = 0.12345}+\bar{\omega}$, where $\bar{\omega}$=**0.00000000000001**. It can be clearly reflected from Figure 9 that the decrypted speech signals are harsh noise without any useful information, and they are completely different from the original speech signals. Therefore, unless the eavesdropper obtains the same decryption keys as the encryption keys, it will be impossible to decrypt and recover the original speech signals or obtain any useful information.

4) REAL-TIME ANALYSIS

It is expected that speech signals can be encrypted and decrypted in real time to meet the real-time requirements of speech secure communication. Still chosen ''Speech Encryption'' (see Figure 6(a)) to test, the encryption time with Algorithm 1 is 0.203574s, and the decryption time with Algorithm 2 is about 0.210356s, which can basically meet the real-time requirements of speech communication.

VI. CONCLUSION

This paper addresses the bipartite synchronization problem of multi-agent systems with signed graph, where the effects of time-varying delay and deception attacks are taken into account. By using a gauge transformation to transform the bipartite synchronization problem of multi-agent systems with signed graph into the traditional synchronization of multi-agent systems with unsigned graph, choosing the appropriate Lyapunov function and applying the Halanay differential inequality, a sufficient condition, which guarantees the bipartite leaderless synchronization for multi-agent systems with unsigned graphs, is newly obtained. When the delayed node-state term or the delayed coupling term is not considered separately, several criteria are established. The effectiveness of the synchronization results is then demonstrated by two numerical examples. Finally, a new multi-agent speech secure communication system is constructed to verify the feasibility of the proposed synchronization results in practical applications.

REFERENCES

[1] R. Olfati-Saber and R. M. Murray, ''Consensus problems in networks of agents with switching topology and time-delays,'' *IEEE Trans. Autom. Control*, vol. 49, no. 9, pp. 1520–1533, Sep. 2004.
[2] Y. Cao, W. Yu, W. Ren, and G. Chen, ''An overview of recent progress in the study of distributed multi-agent coordination,'' *IEEE Trans. Ind. Informat.*, vol. 9, no. 1, pp. 427–438, Feb. 2012.
[3] J. A. Fax and R. M. Murray, ''Information flow and cooperative control of vehicle formations,'' *IEEE Trans. Autom. Control*, vol. 49, no. 9, pp. 1465–1476, Sep. 2004.
[4] W. Ren and E. Atkins, ''Distributed multi-vehicle coordinated control via local information exchange,'' *Int. J. Robust Nonlinear Control*, vol. 1011, no. 17, pp. 1002–1033, 2007.
[5] Z. Qu, J. Wang, and R. A. Hull, ''Cooperative control of dynamical systems with application to autonomous vehicles,'' *IEEE Trans. Autom. Control*, vol. 53, no. 4, pp. 894–911, May 2008.
[6] I. D. Couzin, J. Krause, N. R. Franks, and S. A. Levin, ''Effective leadership and decision-making in animal groups on the move,'' *Nature*, vol. 433, no. 7025, pp. 513–516, 2005.
[7] J. Ren, Q. Song, and G. Lu, ''Event-triggered bipartite leader-following consensus of second-order nonlinear multi-agent systems under signed digraph,'' *J. Franklin Inst.*, vol. 356, no. 12, pp. 6591–6609, Aug. 2019.
[8] F. Heider, ''Attitudes and cognitive organization,'' *J. Psychol.*, vol. 21, no. 1, pp. 107–112, 1946.
[9] D. Cartwright and F. Harary, ''Structural balance: A generalization of Heider's theory,'' *Psychol. Rev.*, vol. 63, no. 5, pp. 277–293, 1956.
[10] S. Majhi, M. Perc, and D. Ghosh, ''Dynamics on higher-order networks: A review,'' *J. Roy. Soc. Interface*, vol. 19, no. 188, Mar. 2022, Art. no. 20220043.

[11] C. Altafini, "Consensus problems on networks with antagonistic interactions," *IEEE Trans. Autom. Control*, vol. 58, no. 4, pp. 935–946, Apr. 2013.
[12] M. E. Valcher and P. Misra, "On the consensus and bipartite consensus in high-order multi-agent dynamical systems with antagonistic interactions," *Syst. Control Lett.*, vol. 66, pp. 94–103, Apr. 2014.
[13] F. A. Yaghmaie, R. Su, F. L. Lewis, and S. Olaru, "Bipartite and cooperative output synchronizations of linear heterogeneous agents: A unified framework," *Automatica*, vol. 80, pp. 172–176, Jun. 2017.
[14] K. Patel and A. Mehta, "Discrete-time sliding mode protocols for leader-following consensus of discrete multi-agent system with switching graph topology," *Eur. J. Control*, vol. 51, pp. 65–75, Jan. 2020.
[15] D. Ye, M.-M. Chen, and H.-J. Yang, "Distributed adaptive event-triggered fault-tolerant consensus of multiagent systems with general linear dynamics," *IEEE Trans. Cybern.*, vol. 49, no. 3, pp. 757–767, Mar. 2019.
[16] X. Xu and L. Gao, "Intermittent observer-based consensus control for multi-agent systems with switching topologies," *Int. J. Syst. Sci.*, vol. 47, no. 8, pp. 1891–1904, Jun. 2016.
[17] Y. J. Zhou, G.-P. Jiang, F.-Y. Xu, and Q.-Y. Chen, "Distributed finite time consensus of second-order multi-agent systems via pinning control," *IEEE Access*, vol. 6, pp. 45617–45624, 2018.
[18] Q. Song, J. Cao, and W. Yu, "Second-order leader-following consensus of nonlinear multi-agent systems via pinning control," *Syst. Control Lett.*, vol. 59, no. 9, pp. 553–562, 2010.
[19] F. Liu, Q. Song, G. Wen, J. Lu, and J. Cao, "Bipartite synchronization of Lur'e network under signed digraph," *Int. J. Robust Nonlinear Control*, vol. 28, no. 18, pp. 6087–6105, Dec. 2018.
[20] Q. Song, G. Lu, G. Wen, J. Cao, and F. Liu, "Bipartite synchronization and convergence analysis for network of harmonic oscillator systems with signed graph and time delay," *IEEE Trans. Circuits Syst. I, Reg. Papers*, vol. 66, no. 7, pp. 2723–2734, Jul. 2019.
[21] D. Meng, "Bipartite containment tracking of signed networks," *Automatica*, vol. 79, pp. 282–289, May 2017.
[22] H. Hu, W. Yu, Q. Xuan, L. Yu, and G. Xie, "Consensus of multi-agent systems in the cooperation–competition network with inherent nonlinear dynamics: A time-delayed control approach," *Neurocomputing*, vol. 158, pp. 134–143, Jun. 2015.
[23] F. Parastesh, K. Rajagopal, S. Jafari, M. Perc, and E. Scholl, "Blinking coupling enhances network synchronization," *Phys. Rev. E, Stat. Phys. Plasmas Fluids Relat. Interdiscip. Top.*, vol. 105, no. 5, 2022, Art. no. 054304.
[24] H.-J. Li, W. Xu, S. Song, W.-X. Wang, and M. Perc, "The dynamics of epidemic spreading on signed networks," *Chaos, Solitons Fractals*, vol. 151, Oct. 2021, Art. no. 111294.
[25] L. Li, J. Lu, and D. W. C. Ho, "Event-based discrete-time multi-agent consensus over signed digraphs with communication delays," *J. Franklin Inst.*, vol. 356, no. 18, pp. 11668–11689, Dec. 2019.
[26] M. Wang, R. Zheng, J. Feng, S. Qin, and W. Li, "Aperiodically intermittent control for exponential bipartite synchronization of delayed signed networks with multi-links," *Chaos: Interdiscipl. J. Nonlinear Sci.*, vol. 30, no. 3, 2020, Art. no. 033110.
[27] Y. Cui, Y. Liu, W. Zhang, and F. E. Alsaadi, "Sampled-based consensus for nonlinear multiagent systems with deception attacks: The decoupled method," *IEEE Trans. Syst., Man, Cybern., Syst.*, vol. 51, no. 1, pp. 561–573, Jan. 2021.
[28] W. He, X. Gao, W. Zhong, and F. Qian, "Secure impulsive synchronization control of multi-agent systems under deception attacks," *Inf. Sci.*, vol. 459, pp. 354–368, Aug. 2018.
[29] G. Wen, X. Zhai, Z. Peng, and A. Rahmani, "Fault-tolerant secure consensus tracking of delayed nonlinear multi-agent systems with deception attacks and uncertain parameters via impulsive control," *Commun. Nonlinear Sci. Numer. Simul.*, vol. 82, Mar. 2020, Art. no. 105043.
[30] J. Hu and W. X. Zheng, "Emergent collective behaviors on coopetition networks," *Phys. Lett. A*, vol. 378, nos. 26–27, pp. 1787–1796, 2014.
[31] D. Meng, M. Du, and Y. Jia, "Interval bipartite consensus of networked agents associated with signed digraphs," *IEEE Trans. Autom. Control*, vol. 61, no. 12, pp. 3755–3770, Dec. 2016.
[32] P. Wang, G. Wen, X. Yu, W. Yu, and Y. Wan, "Synchronization of resilient complex networks under attacks," *IEEE Trans. Syst., Man, Cybern., Syst.*, vol. 51, no. 2, pp. 1116–1127, Feb. 2021.
[33] J. Lu, D. W. C. Ho, J. Cao, and J. Kurths, "Exponential synchronization of linearly coupled neural networks with impulsive disturbances," *IEEE Trans. Neural Netw.*, vol. 22, no. 2, pp. 329–336, Feb. 2011.
[34] W. Ren and R. W. Beard, "Consensus seeking in multiagent systems under dynamically changing interaction topologies," *IEEE Trans. Autom. Control*, vol. 50, no. 5, pp. 655–661, May 2005.
[35] Y. Zhang and Y.-P. Tian, "Consentability and protocol design of multi-agent systems with stochastic switching topology," *Automatica*, vol. 45, no. 5, pp. 1195–1201, May 2009.
[36] C. T. H. Baker and E. Buckwar, "Exponential stability in p-th mean of solutions, and of convergent Euler-type solutions, of stochastic delay differential equations," *J. Comput. Appl. Math.*, vol. 184, no. 2, pp. 404–427, Dec. 2005.
[37] L. Zhang and Y. Yang, "Impulsive effects on bipartite quasi synchronization of extended caputo fractional order coupled networks," *J. Franklin Inst.*, vol. 357, no. 7, pp. 4328–4348, May 2020.
[38] J. Fu, G. Wen, W. Yu, T. Huang, and J. Cao, "Exponential consensus of multiagent systems with Lipschitz nonlinearities using sampled-data information," *IEEE Trans. Circuits Syst. I, Reg. Papers*, vol. 65, no. 12, pp. 4363–4375, Jun. 2018.

YANSEN LIU was born in Yangzhou, China, in 1998. He received the B.Eng. degree from the School of Electrical Engineering, Nantong University, Nantong, China, in 2020, where he is currently pursuing the M.Sc. degree. His current research interest includes consensus problem of multi-agent systems.

SUYING SHENG received the B.E. degree in electrical engineering and automation from Nantong University, Nantong, in 2003, the M.S. degree in communication and information system from Soochow University, Suzhou, in 2006, and the Ph.D. degree in information and communication engineering from Nantong University, in 2020. She has been with the School of Electrical Engineering, Nantong University, since 2006, where she is currently a Senior Experimentalist. Her current research interests include distributed estimation over sensor networks, dynamical networks complex, and fuzzy systems.

JIAHAO ZHANG was born in Nantong, China, in 1998. He received the B.Eng. degree in electrical engineering and automation from the School of Electrical Engineering, Nantong University, Nantong, in 2020, where he is currently pursuing the M.Sc. degree. His current research interest includes bipartite synchronization under signed digraph.

GUOPING LU received the B.S. degree from the Department of Applied Mathematics, Chengdu University of Science and Technology, China, in 1984, and the M.S. and Ph.D. degrees from the Department of Mathematics, East China Normal University, China, in 1989 and 1998, respectively. He is currently a Professor at the School of Electrical Engineering, Nantong University, Jiangsu, China. His current research interests include singular systems, robust control, and networked control.